

 Open access • Journal Article • DOI:10.1063/1.1640789

## Excimer emission from cathode boundary layer discharges — [Source link](#)





M. Moselhy, Karl H. Schoenbach

**Published on:** 30 Jan 2004 - Journal of Applied Physics (American Institute of Physics)

**Topics:** Cathode, Xenon, Anode, Atmospheric pressure and Excimer

Related papers:

- [Self-organization in cathode boundary layer microdischarges](#)
- [Self-organization in cathode boundary layer discharges in xenon](#)
- [Direct current planar excimer source](#)
- [Predicted properties of microhollow cathode discharges in xenon](#)
- [High-Pressure Microdischarges: Sources of Ultraviolet Radiation](#)

Share this paper:    

View more about this paper here: <https://typeset.io/papers/excimer-emission-from-cathode-boundary-layer-discharges-su7931d0u7>

2004

# Excimer Emission From Cathode Boundary Layer Discharges

Mohamed Moselhy  
*Old Dominion University*

Karl H. Schoenbach  
*Old Dominion University*

Follow this and additional works at: [https://digitalcommons.odu.edu/bioelectrics\\_pubs](https://digitalcommons.odu.edu/bioelectrics_pubs)

Part of the [Electrical and Computer Engineering Commons](#), [Plasma and Beam Physics Commons](#), and the [Polymer Chemistry Commons](#)

---

## Repository Citation

Moselhy, Mohamed and Schoenbach, Karl H., "Excimer Emission From Cathode Boundary Layer Discharges" (2004). *Bioelectrics Publications*. 236.  
[https://digitalcommons.odu.edu/bioelectrics\\_pubs/236](https://digitalcommons.odu.edu/bioelectrics_pubs/236)

## Original Publication Citation

Moselhy, M., & Schoenbach, K. H. (2004). Excimer emission from cathode boundary layer discharges. *Journal of Applied Physics*, 95(4), 1642-1649. doi:10.1063/1.1640789

# Excimer emission from cathode boundary layer discharges

Mohamed Moselhy and Karl H. Schoenbach<sup>a)</sup>

*Physical Electronics Research Institute, Old Dominion University, Norfolk, Virginia 23529*

(Received 28 August 2003; accepted 19 November 2003)

The excimer emission from direct current glow discharges between a planar cathode and a ring-shaped anode of 0.75 and 1.5 mm diameter, respectively, separated by a gap of 250  $\mu\text{m}$ , was studied in xenon and argon in a pressure range from 75 to 760 Torr. The thickness of the “cathode boundary layer” plasma, in the 100  $\mu\text{m}$  range, and a discharge sustaining voltage of approximately 200 V, indicates that the discharge is restricted to the cathode fall and the negative glow. The radiant excimer emittance at 172 nm increases with pressure and reaches a value of 4  $\text{W}/\text{cm}^2$  for atmospheric pressure operation in xenon. The maximum internal efficiency, however, decreases with pressure having highest values of 5% for 75 Torr operation. When the discharge current is reduced below a critical value, the discharge in xenon changes from an abnormal glow into a mode showing self-organization of the plasma. Also, the excimer spectrum changes from one with about equal contributions from the first and second continuum to one that is dominated by the second continuum emission. The xenon excimer emission intensity peaks at this discharge mode transition. In the case of argon, self-organization of the plasma was not seen, but the emission of the excimer radiation (128 nm) again shows a maximum at the transition from abnormal to normal glow. As was observed with xenon, the radiant emittance of argon increases with pressure, and the efficiency decreases. The maximum radiant emittance is 1.6  $\text{W}/\text{cm}^2$  for argon at 600 Torr. The maximum internal efficiency is 2.5% at 200 Torr. The positive slope of the current–voltage characteristics at maximum excimer emission in both cases indicates the possibility of generating intense, large area, flat excimer lamps.

© 2004 American Institute of Physics. [DOI: 10.1063/1.1640789]

## I. INTRODUCTION

Efficient excimer generation in rare gas and rare gas–halide gas discharge plasmas requires nonequilibrium discharges, operated at high pressure. Examples for such nonequilibrium discharges are dielectric barrier discharges,<sup>1</sup> corona discharges,<sup>2</sup> and microhollow cathode discharges (MHCDs).<sup>3–5</sup> Microhollow cathode discharges are dc or pulsed gas discharges between two electrodes, separated by a dielectric, and containing a concentric hole. The hole diameter in such a hollow cathode configuration is in the hundred-micrometer range. The high energy electrons in such a hollow cathode discharge, required to provide a high concentration of excited or ionized rare gas atoms, and the high pressure operation, which favors excimer formation, a three-body process, make these discharges efficient excimer radiation sources. The excimer efficiency of MHCDs in Xe, Ar, He, Ne, XeCl, and ArF ranges from 1% to 20%.<sup>3,4,6–8</sup>

When operating these discharges in xenon<sup>9</sup> or argon,<sup>10</sup> it was noticed that the discharge plasma, with increasing current, extended beyond the microhole and began to cover the plane area of the cathode surrounding the microhole. The discharge voltage did not change during this phase. This discharge characteristic is typical for normal glow discharges. The voltage increased with current only when the plasma layer had covered the entire open cathode area and reached the edge of the dielectric, a characteristic of abnormal glow discharges. This normal glow and abnormal glow structure of

the discharge was found to be independent of the presence of the microhole.<sup>11</sup>

In order to study the planar plasma layer in xenon and argon discharges, particularly its excimer emission, we have eliminated the microhole. The electrode configuration now consists of a planar cathode, separated from a ring-shaped anode by a dielectric with an opening of the same diameter as the anode (Fig. 1). The diameter of the opening is in the range of fractions of millimeters to several millimeters. Experimental studies (measurements of the current–voltage characteristics and photographs in the visible range) of argon discharges in such an electrode configuration have shown that such discharges are stable up to pressures of 760 Torr.<sup>12</sup>

The discharge in such an electrode configuration seems to be reduced to the cathode fall and the negative glow with the negative glow serving as a planar “anode,” providing a current path for the cathode fall current to the ring-shaped metal anode (Fig. 1).<sup>11</sup> This assumption is supported by earlier measurements, which showed the thickness of the xenon plasma layer being in the range from 100 to 150  $\mu\text{m}$  for pressures of 200 Torr.<sup>9</sup> We have not found cathode fall and negative glow data for xenon discharges between molybdenum electrodes; however, thickness values on the order of 100  $\mu\text{m}$  are typical for noble gases in this pressure range.<sup>13</sup> We will, because of the structure of this discharge, refer to it in the following as the cathode boundary layer (CBL) discharge. Experiments in xenon with this electrode configuration have shown that such discharges, when operated in a certain current range, show pattern formation.<sup>11</sup>

<sup>a)</sup>Electronic mail: schoenbach@ece.odu.edu

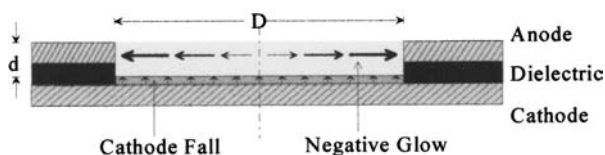


FIG. 1. CBL discharge electrode geometry and estimated current density pattern (see Ref. 11).

Although this configuration is much different from a hollow cathode discharge, the cathode boundary layer discharge is expected to have a similar, nonthermal electron energy distribution. Measurements of the electron energy distribution in the cathode fall of a low-pressure helium glow discharge between plane-parallel electrodes by Gill and Webb<sup>14</sup> have shown that the electron energy distribution contains electrons with energies up to values that correspond to the cathode fall voltage. This and the stable high-pressure operation of CBL discharges have led us to expect that the excimer emission from such discharges is comparable to that from microhollow cathode discharges.

## II. EXPERIMENTAL SETUP

The electrodes consist of a planar cathode (molybdenum, 250  $\mu\text{m}$  thick) and a ring-shaped anode (molybdenum, 250  $\mu\text{m}$  thick) separated by a dielectric (alumina, 250  $\mu\text{m}$  thick) with the same opening diameter as the anode (Fig. 1). The inner diameter of the ring-shaped anode was 0.75 mm for the experiments in xenon and 1.5 mm for those in argon. The discharge chamber was evacuated to a pressure in the mTorr range and filled with xenon or argon up to pressures ranging from 75 Torr to atmospheric pressure. While the discharges in xenon were operated in a static mode, in argon the gas was flowed across the electrode wafer to reduce the effects of impurities emitted from the electrode or dielectric or entering the discharge chamber through minor leaks. The flow rate of 160 sccm was controlled by a mass flow controller (UFC-8160, Coastal Instruments). Flowing the gas was found in an earlier study to reduce the effect of oxygen on the excimer emission.<sup>15</sup> Under static conditions the strong atomic oxygen line emission at 130.5 nm, which is due to resonant energy transfer with argon excimers, or precursors of such excimers, was found to dominate the excimer emission of argon, which peaks at 128 nm.

For the studies described in the following, the discharges were operated in the dc mode. The dc current was measured by means of a current viewing resistor (CVR) of 1 k $\Omega$  in series with the discharge, and the voltage was measured across the discharge and the CVR. The discharge voltage was obtained by subtracting the voltage across the CVR from the measured voltage.

Images of the CBL discharges were recorded in the visible and vacuum-ultraviolet (VUV) spectral range. In the visible range a charge coupled device (CCD) camera was used in combination with a microscope lens to record the discharge images (end-on) dependent on current and pressure. For the VUV images, an intensified CCD camera (ICCD-MAX, Roper Scientific) was used in combination with an optical filter having a peak transmission of 24% at 170.9 nm,

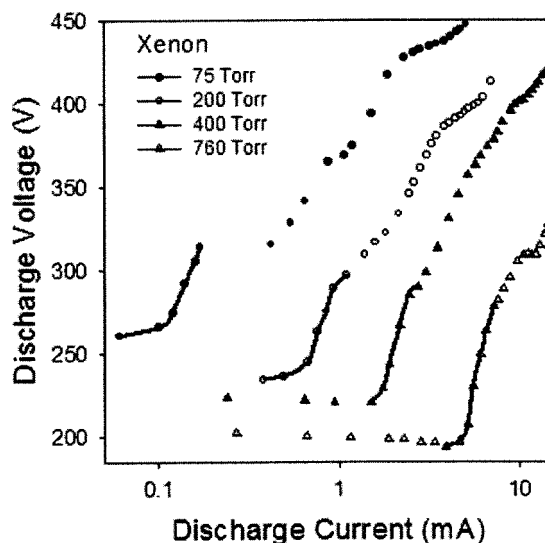


FIG. 2. Voltage-current characteristics of xenon CBL discharges with pressure as parameter. The cathode diameter is 0.75 mm. The current range for which self-organization of the plasma is observed is indicated by bold lines connecting the data points.

a full width at half maximum (FWHM) of 26.8 nm, and a  $\text{Mg}_2\text{F}$  lens.<sup>9</sup> The system was adjusted to magnify the image of the discharge by a factor of 6. The entire imaging system, including lens and optical filter, was placed under vacuum to avoid absorption in air. The same setup was used for VUV imaging of argon discharges. In this case, the optical filter has a peak transmission of 20.7% at 125 nm and a FWHM of 14.5 nm.

The spectral distribution of the excimer emission from xenon and argon was recorded using a 0.2 m vacuum monochromator (McPherson, model 302) with a holographic grating and a photomultiplier tube (Hamamatsu, model R1533). The wavelength range was set at 130–200 nm for xenon (172 nm) and 110–160 nm for argon (128 nm). Since we were mainly interested in the excimer continuum, rather than line emission from impurities, we have set the width of the entrance slit of the spectrograph such that the spectral resolution was only 1 nm. For absolute power measurements, a calibrated radiometer (IL1400) with a calibrated detector (SED185) was used for xenon<sup>16</sup> and a calibrated photodiode (SXUV-100, International Radiation Detectors, Inc.) was used for argon.<sup>15</sup> In these measurements the excimer source was assumed to be a point source with isotropic emission.<sup>16</sup>

## III. RESULTS

### A. Xenon

For CBL discharges operated in xenon, the dc voltage and current were recorded for pressures of 75, 200, 400, and 760 Torr. The voltage-current ( $V$ - $I$ ) characteristic (Fig. 2) showed a different behavior from that of MHCDs. While in MHCDs the  $V$ - $I$  characteristics are dominated by a negative differential resistance range<sup>17</sup> due to the hollow cathode effect, the  $V$ - $I$  characteristic for CBL discharges is mainly resistive (positive slope of  $V$ - $I$  characteristic) (Fig. 2). The voltage stayed constant only when the discharge was operated at low current levels indicating a normal glow dis-

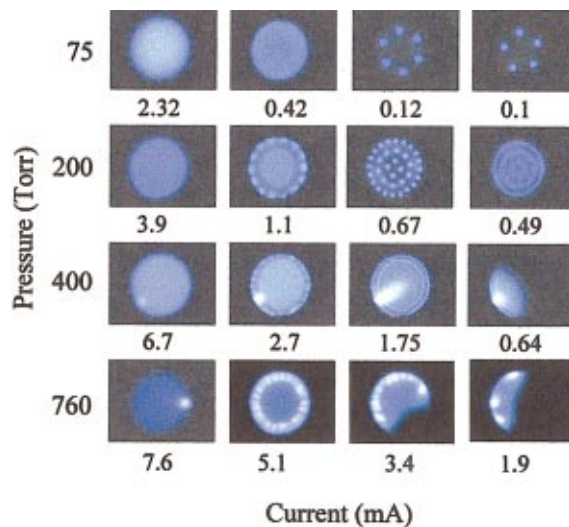


FIG. 3. (Color) End-on images of CBL xenon discharges in the visible dependent on pressure and current. The diameter of the cathode is 0.75 mm. The brightness of the images at 75, 200, and 400 Torr is for all currents (except the largest one) increased relative to that at 760 Torr, in order to better show the pattern structure.

charge. The sustaining voltage in this mode decreases with pressure, from more than 250 V at 75 Torr to less than 200 V at 760 Torr.

This current range, which was identified in an earlier publication as a range with self-organization of the plasma,<sup>11</sup> is followed by a  $V$ - $I$  characteristic with a smaller, but still positive, slope. In this range, the discharge is in an abnormal glow mode as also indicated by the end-on images of the plasma (Fig. 3). The current at the transition from the abnormal glow mode to the self-organization mode and normal glow mode, respectively, is proportional to the square of the pressure. This is typical for a normal glow discharge at the transition to the abnormal glow discharge when the plasma has just covered the entire cathode area.

End-on images (Fig. 3) in the visible range of spectrum show the plasma structure dependent on both pressure and current. When the discharge is operated at high current, it covers the entire cathode area, typical for an abnormal glow discharge. With decreasing current the plasma changes from a homogenous emitter to one with a rotationally symmetric pattern. Generally, with increasing pressure, the current range where the patterns appear shifts to higher currents; the patterns lose their symmetry and the structure becomes denser. The emission patterns were, particularly in the low-pressure range, found to change in steps. The decrease in current required to change the configuration is rather small. It needs to be noted that this process could only be observed when the current was lowered. When attempts were made to change the discharge pattern by increasing the current, the discharge simply extinguished.

With further reduction of current, these patterns become more distinct, and cover less and less of the available cathode surface. If we assume that the luminosity of the plasma is proportional to the current density, the current density in the luminous filaments would assume an almost constant value of approximately  $0.3 \text{ A/cm}^2$ . Further reduction of cur-

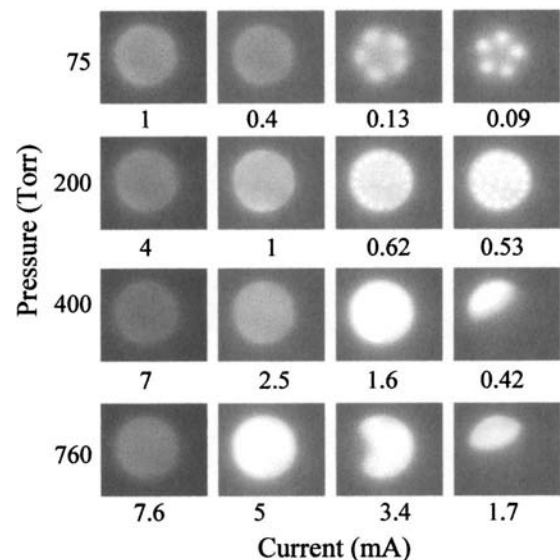


FIG. 4. VUV end-on images of CBL discharges in xenon at 172 nm dependent on pressure and current. The diameter of the cathode is 0.75 mm.

rent at higher pressures ( $>400$  Torr) causes the loss of symmetry in these patterns until the discharge extinguishes. This phase corresponds to the normal glow discharge characteristics as shown in Fig. 2.

Similar to the visible images, end-on VUV images of xenon discharges (Fig. 4) showed a uniform plasma filling the entire cathode area at currents above the threshold for abnormal glow discharges. The current values of these discharges are not identical to those shown in Fig. 3. The main goal here was to demonstrate the change at a given pressure as the current is varied, and not so much a direct visible to VUV comparison. When the current is lowered below this threshold, the plasma shows similar spatial structures as observed in the visible; however, they appear less distinct. The strong decrease in intensity when the discharge is operated in the abnormal glow mode, at high current values is surprising.

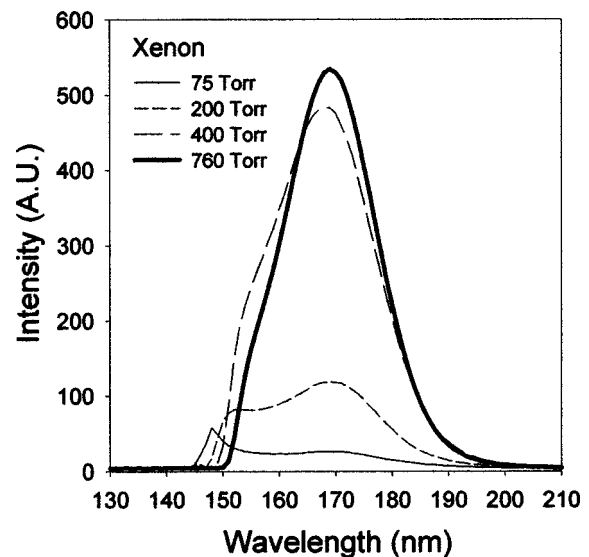


FIG. 5. Spectral emission of xenon CBL discharges at a constant current of 2 mA, with pressure as parameter.



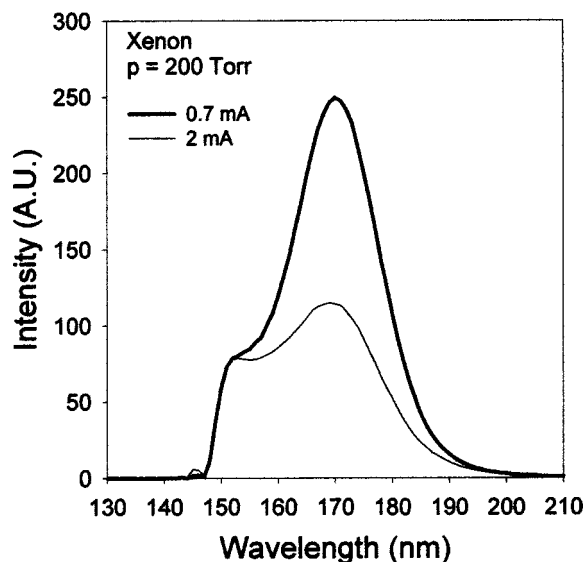


FIG. 6. Current dependence of the excimer emission of xenon CBL discharges at a pressure of 200 Torr. The spectral emission for a current of 0.7 mA corresponds to the self-organized mode, the emission at 2 mA to the abnormal glow mode.

This is very clearly seen at 400 Torr in the drop in intensity when the current is increased from 1.6 to 2.5 mA (Fig. 4). Again, as seen in the visible, when reducing the current, the discharge either transfers into the patterned mode (at low pressure) or into the normal glow mode (at high pressures), where only part of the cathode area is covered with a plasma layer.

The spectral distribution of the xenon excimer radiation was recorded for the four pressure values (75, 200, 400, and 760 Torr). Figure 5 shows xenon excimer spectra at a constant current of 2 mA. The intensity increases with increasing pressure as expected, due to the increase in the rate of excimer formation, a three-body process, with pressure. Also expected is the observed shift in the spectral distribution from the first to the second continuum, when the pressure is increased as has been observed in dielectric barrier discharge.<sup>18</sup> This effect is due to the increase in the population of the  $3\Sigma_u^+$  molecular state at higher pressure at the expense of the  $1\Sigma_u^+$  molecular state.<sup>18</sup>

Also interesting is the change in the spectral distribution at the same pressure, but for current values that correspond to different discharge modes. An example is shown in Fig. 6, where the spectra are shown for a 200 Torr xenon discharge. The spectrum at a current of 2 mA corresponds to the abnormal glow mode and that at 0.7 mA corresponds to the self-organization mode. Although the first continuum intensity remained the same when the current was changed from 0.7 to 2 mA, the second continuum intensity decreased to about half of that at 0.7 mA.

In order to measure the absolute value of the emitted excimer radiation, a calibrated detector was used.<sup>16</sup> The output excimer power was measured as a function of both current and pressure and the result was found to be consistent with that obtained from the VUV images (Fig. 4). At low current, while the voltage is constant, the intensity increases with increasing current, as shown in Fig. 7. This increase in

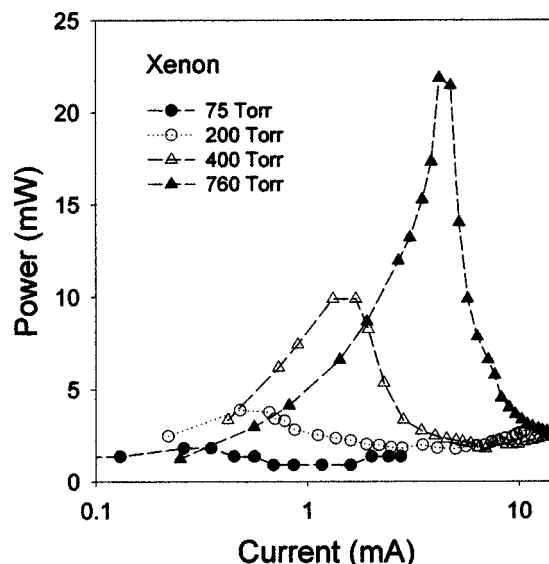


FIG. 7. Absolute values of the excimer emission for CBL discharges in xenon, dependent on current, with pressure as parameter.

intensity with current is due to the increasing discharge area typical for the normal glow discharge mode. When the current exceeds a certain value, related to the transition from normal to abnormal glow (at higher pressures), or the transition from patterned structures to abnormal glow at lower pressures, the excimer power decreases dramatically. The maximum in emission shifts, with increasing pressure, to higher current, and increases in amplitude.

Whereas the excimer power increases with increasing pressure, the maximum internal excimer efficiency decreases with increasing pressure (Fig. 8). The internal efficiency, the ratio of the output optical power to the input electrical power, was calculated based on the results of the absolute measurements. While the discharge is in the normal glow mode, the efficiency is almost constant, independent of current. It decreases when the current exceeds the critical value at which

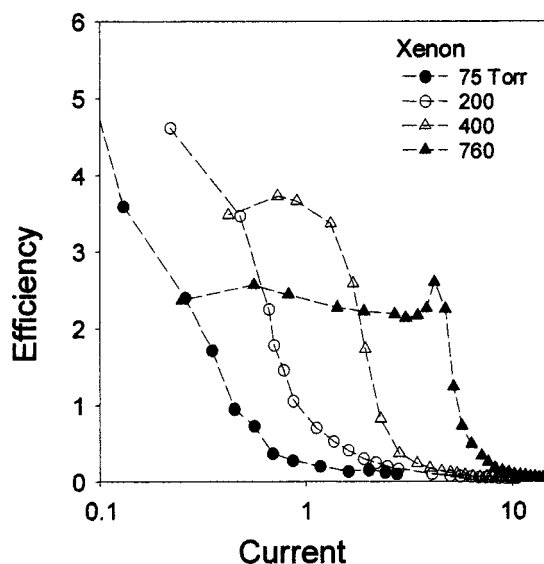


FIG. 8. Internal efficiency of CBL discharges in xenon dependent on discharge current with pressure as parameter.

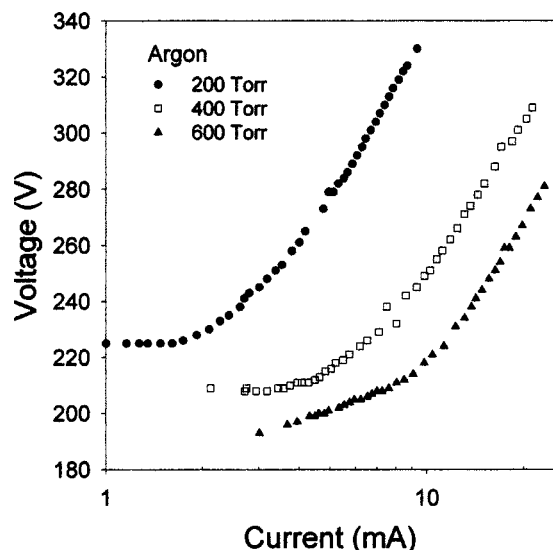


FIG. 9. Voltage-current characteristics for CBL discharges in argon with pressure as parameter. The cathode diameter is 1.5 mm.

the discharge transfers into the abnormal glow mode. The maximum efficiency is in the range of 2%–5% depending on the gas pressure, with largest values at lowest pressures.

### B. Argon

The same studies that were performed with xenon as excimer gas were performed with argon. Whereas xenon excimer radiation peaks at 172 nm, argon excimer emission peaks at 128 nm, and therefore requires a different calibration system, as described in Sec. II. The electrode configuration was similar to that used for the xenon studies, except that the cathode opening was 1.5 mm rather than 0.75 mm.

Similar to xenon, the  $V$ - $I$  characteristic for CBL discharges in argon shows a range of constant voltage for low currents and a resistive behavior at higher currents (Fig. 9). Again, this indicates a normal glow at low current and abnormal glow mode at higher current. In contrast to the xenon

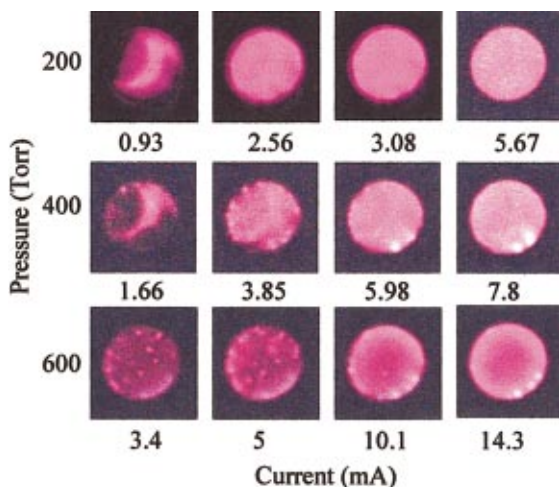


FIG. 10. (Color) End-on images of CBL discharges in argon in the visible, dependent on pressure and current. The cathode diameter is 1.5 mm.

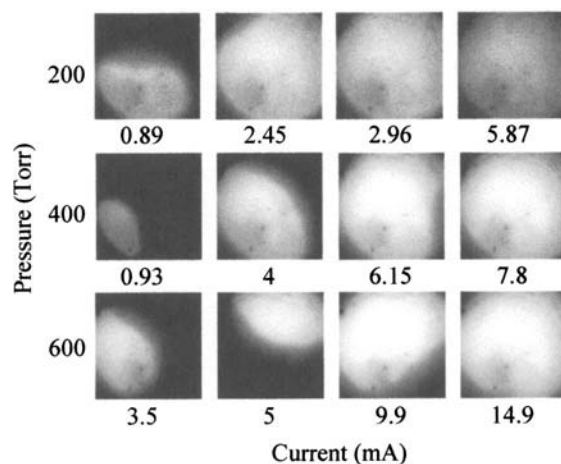


FIG. 11. End-on VUV images of CBL discharges in argon dependent on pressure and current. The cathode diameter is 1.5 mm.

$V$ - $I$  curves, the argon  $V$ - $I$  curves are less structured. The transition from normal glow to abnormal glow is smoother.

End-on images of argon CBL discharges in the visible range are shown in Fig. 10. Unlike images of xenon CBL discharges, there is no pattern formation. Regions of increased intensity at high current are assumed to be due to cathode surface irregularities since their location is independent of current. The structure of the two discharge modes, the normal glow, where the cathode surface is only partially covered with plasma, to the abnormal glow, with the entire cathode area covered, is clearly visible.

Using the same VUV imaging system as for xenon, images of the excimer emission were recorded, in this case at 128 nm (Fig. 11). The images, similar to the images in the visible, show no structure, except what is assumed regions of lower intensity due to cathode surface nonhomogeneities. However, as for the case of xenon, the intensity of the emission decreased when the discharge transferred from normal

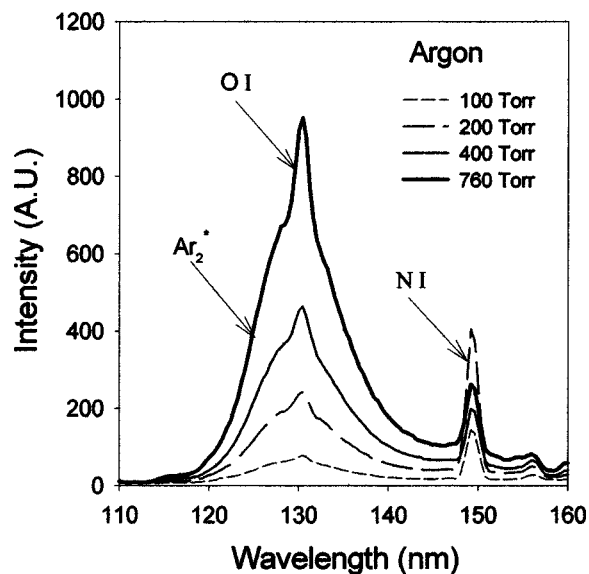


FIG. 12. Spectral emission of argon CBL discharges at constant current of 3 mA with pressure as parameter.

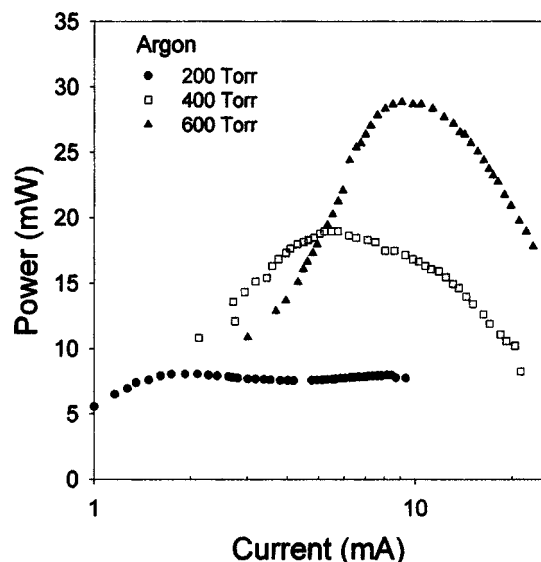


FIG. 13. Excimer power from CBL discharges in argon dependent on current with pressure as parameter.

glow into abnormal glow. This is clearly visible in Fig. 11, for the pressure of 200 Torr, with the current varying from 2.45 to 5.87 mA.

The argon spectrum between 110 and 160 nm is shown in Fig. 12 for pressures of 100, 200, 400, and 760 Torr, and a current of 3 mA. The intensity of the excimer emission at 128 nm increases with increasing pressure as in the case of xenon. In spite of using flowing argon, however, there is still atomic oxygen emission at 130.5 nm<sup>15</sup> and, at 149 nm, a strong nitrogen line emission [ $2s^2 2p^3 - 2s^2 2p^2(^3P)3s$ ] is observed indicating air leaks in the discharge chamber. The nitrogen line width in the recorded spectrum (Fig. 12) is determined by the resolution of the monochromator. Whereas the intensity of the oxygen line increases with pressure, the nitrogen line does not follow this pattern. It has a maximum

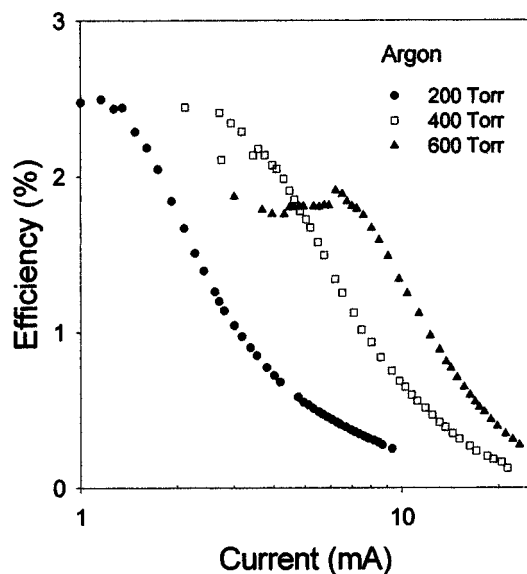


FIG. 14. Excimer efficiency from CBL discharges in argon dependent on current with pressure as parameter.

at a pressure of 200 Torr, and its intensity decreases with higher pressure. This is not surprising, since the atomic oxygen emission at 130.5 nm is correlated with the argon excimer concentration,<sup>15</sup> whereas the nitrogen emission is likely to be related to leaks in the discharge chamber, which at higher pressure (at a reduced pressure difference between outside and inside of the chamber) affect the gas concentration less and less.

In argon, a calibrated photodiode (SXUV-100) was used to measure the absolute excimer power at 128 nm. As in xenon, the measured power increases with the current up to a maximum and begins to decrease when the current reaches a value at which the discharge switches from normal to abnormal glow mode (Fig. 13). The efficiency, obtained from the  $V-I$  characteristics and the absolute values of the excimer emission, was found, like xenon, to have a maximum at currents at the transition from normal to abnormal glow (Fig. 14). The maximum efficiency was in the range of 1.5%–2.5% when the pressure was varied between 600 and 200 Torr.

#### IV. DISCUSSION

The CBL discharge is a type of high-pressure glow discharge, which is restricted to the cathode fall and negative glow, with the negative glow serving as a virtual anode: the plasma in the negative glow region provides a radial current path to the ring-shaped metal anode. This assumption is not only supported by the measured thickness of the plasma layer<sup>9</sup> which corresponds to the thickness of cathode fall plus negative glow, but also by the measured sustaining voltage. For high-pressure operation in both gases, the pressure in the normal glow mode was measured as approximately 200 V (Fig. 2 for xenon and Fig. 9 for argon). The equation for the cathode fall voltage is<sup>19</sup>

$$V_c = \frac{14.5B}{2A} \ln \left( 1 + \frac{1}{\gamma} \right) \quad (1)$$

with values of  $A = 26 \text{ (cm Torr)}^{-1}$  and  $B = 350 \text{ V/(cm Torr)}$  for xenon<sup>20</sup> and  $A = 13.6 \text{ (cm Torr)}^{-1}$  and  $B = 235 \text{ V/(cm Torr)}$  for argon.<sup>13</sup> The secondary electron emission coefficient,  $\gamma$ , depends on the type of gas, the electrode material, and the electrode surface. According to data listed in Ref. 13, typical values for  $\gamma$  are in the range from 0.05 to 0.3. For a secondary electron coefficient in this range, the cathode fall voltage was calculated to vary between 140 and 300 V for xenon and 180 and 380 V for argon. The calculated voltage is in the range of the measured sustaining voltage of the discharge, assuming that the voltage across the negative glow is negligible.

The current density in the radial direction,  $J_r$ , assuming a homogeneous current density in the direction normal to the cathode,  $J_z$ , is given as<sup>11</sup>

$$J_r = J_z \left( \frac{r}{2d} \right) \quad (2)$$

with  $d$  being the diameter of the anode, and  $r$  being the radial position. This increase in current density with radius, ex-



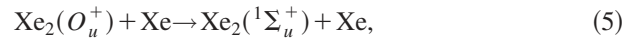
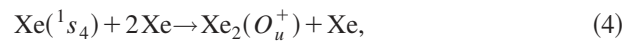
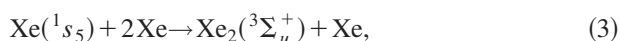
plains the fact that nonhomogeneities develop first at the edges of the cathode (Fig. 3 for xenon and Fig. 10 for argon).

The current density in the cathode fall of these CBL discharges has been shown, for xenon, to reach, or even exceed, values of 2 A/cm<sup>2</sup>, and only slightly less for argon. Critical current densities for the onset of instabilities for atmospheric pressure discharges are cited in a review paper on the “generation of large-volume, atmospheric-pressure non-equilibrium plasmas” by Kunhardt<sup>21</sup> as 10 mA/cm<sup>2</sup>. However, it needs to be noted that these values are related to air discharges rather than rare gas discharges.<sup>22</sup> The stability of CBL discharges, which allows us to operate them in a dc mode, is assumed to be due to thermal losses through the cathode foil, an effect that we also consider to be the reason for the observed self-organization in xenon discharges.<sup>11</sup> If this assumption can be experimentally confirmed, forced cooling of the cathode foil will allow us to extend stability of these dc discharges to even higher current densities.

Self-organization has been observed in xenon discharges but not in argon discharges at comparable pressures and current densities. The computed second stable branch of current density–voltage characteristics, for glow discharges with strong thermal losses to the cathode, depends strongly on the transport parameters of the gas, ionization coefficient, and the secondary electron coefficient.<sup>11</sup> It is therefore likely that, for argon, the parameter range for self-organization is situated outside the parameter range which is covered in this study. Further experiments over a wider parameter range with controlled cathode temperatures are needed to test our hypothesis.

The medium and high-pressure dc discharges in both xenon and argon emit excimer radiation with efficiencies reaching values of almost 5% in xenon, and 2.5% in argon. This is lower by a factor of 1.5 than that for dc MHCDs in xenon<sup>16</sup> and by a factor of 2.4 than that for dc MHCDs in argon.<sup>10</sup> However, the advantages of CBL discharges, i.e., the simple design and the resistive characteristics, could outweigh the higher efficiency of MHCD discharges when it comes to applications such as excimer lamps. For xenon, and to a lesser extent for argon, the efficiency increases when the pressure is reduced from atmospheric pressure to pressures on the order of 100 Torr. One would assume, based on the importance of three-body collisions in the formation of the excimer, that the efficiency increases rather than decreases with pressure. What is also surprising is the fact that the efficiency decreases strongly with current above the transition from normal glow to abnormal glow. This change in efficiency, and also in power density (Fig. 7 for xenon and Fig. 13 for argon) with current is, for xenon, correlated to strong changes in the spectral distribution. As shown in Fig. 6, when increasing the current from 0.7 to 2 mA at a pressure of 200 Torr, the second continuum decreases strongly, whereas the first continuum stays approximately the same. This change in current corresponds to a transition from the range where we see self-organization to a range with homogeneous emission as shown in Figs. 3 and 4.

The reactions that control the excimer generation are<sup>23</sup>



where the metastable state designation uses the Paschen notation.  $\text{Xe}(^1s_5)$  and  $\text{Xe}(^1s_4)$  are xenon excited states, the precursors for excimers. The second continuum arises from the radiative decay of the low-lying vibrational levels of the lower lying triplet state,  $\text{Xe}_2(^3\Sigma_u^+)$ , whereas the first continuum arises from the decay of the vibrationally excited levels of the higher-lying singlet state,  $\text{Xe}_2(^1\Sigma_u^+)$ . The rate coefficients for reactions (3), (4), and (5) are  $7.03 \times 10^{-44} \text{ m}^6 \text{ s}^{-1}$ ,<sup>24</sup>  $5.3 \times 10^{-44} \text{ m}^6 \text{ s}^{-1}$ , and  $7 \times 10^{-17} \text{ m}^3 \text{ s}^{-1}$ ,<sup>25</sup> respectively. For rare gas excimer formation via electron-impact ionization, recombination is a rate-limiting process, as it has a cross section which peaks for electrons with energies close to zero. In an electron energy distribution determined by the cathode fall of the glow discharge, the density of such low energy electrons is likely to be small. Disregarding this pathway to excimer formation, the intensity of the first continuum emission is determined by the population of the  $\text{Xe}(^1s_4)$  state, whereas the population of the second continuum is determined by the population of the  $\text{Xe}(^1s_5)$  state.

The fractional production rates of the two levels,  $\text{Xe}(^1s_5)$  and  $\text{Xe}(^1s_4)$ , are strongly dependent on the electron temperature.<sup>23</sup> For equilibrium conditions this dependence can be expressed in terms of the reduced electric field,  $E/N$ , with  $N$  being the gas density. With increasing electron energy or reduced electric field, the fractional production rate of the  $\text{Xe}(^1s_4)$  level increases and that of the  $\text{Xe}(^1s_5)$  level decreases. The crossover value is 15% at an electron energy of 5 eV. This means that with increasing electron energy and reduced electric field, the second continuum decreases.

The observed change in the spectral distribution may therefore be due to either an increase in electron energy or a reduction in gas density due to heating. The transition from the normal to the abnormal cathode fall causes a reduction in cathode fall thickness and a simultaneous increase in cathode fall voltage, which will result in an increase in electron energy. Also, the increased energy deposition in the cathode fall may lead to an increase in gas temperature and consequently to a reduction in gas density. The increase in gas temperature would also explain the reduction in efficiency<sup>26</sup> at the transition from normal to abnormal cathode fall in both gases. Modeling of the excimer kinetics in both gases, as was done for barrier discharges,<sup>23</sup> is required for a better understanding of the excimer kinetics in CBL discharges, a task beyond the scope of this article.

An important feature of CBL discharges is the positive slope in the voltage–current characteristics over most of the current range, except for low current values (Fig. 2 for xenon and Fig. 9 for argon). This shows that parallel operation of these discharges is possible without using individual ballast resistors. A consequence of this resistive discharge behavior is the possibility of constructing large area, thin (100  $\mu\text{m}$ ) plasma sources, and consequently, large area VUV emitters at pressures up to and even exceeding atmospheric pressure. For example when xenon is operated at a pressure of 400

Torr and a current of 1 mA the efficiency is approximately 4% (Fig. 8). The efficiency is an internal efficiency assuming isotropic emission, and consequently no more than half of the emitted light will reach the observer. For a 1 mA xenon discharge, at a discharge voltage of 225 V, the electric power density is  $50 \text{ W/cm}^2$ ; with an internal efficiency of 4% the intensity of the excimer radiation at 172 nm is consequently  $1 \text{ W/cm}^2$ . For argon at 400 Torr and 5 mA, a similar calculation gives us an electrical power density of  $60 \text{ W/cm}^2$  and an intensity of  $0.5 \text{ W/cm}^2$ . The intensity can be increased even further by increasing the gas pressure (Figs. 7 and 13), but at the expense of efficiency. However, the simple electrode configuration makes effective cooling of the cathode foil possible, and therefore allows extending the application of CBL discharges to very intense, large area excimer lamps.

## ACKNOWLEDGMENTS

This work is supported by NSF (CTS-0078618 and INT-0001438). The authors wish to thank Javed Ansari for his help in performing the measurements in argon.

- <sup>1</sup>B. Eliasson and U. Kogelschatz, IEEE Trans. Plasma Sci. **19**, 309 (1991).
- <sup>2</sup>A. K. Shuaibov, A. I. Minya, and A. I. Dashchenko, Tech. Phys. **46**, 1582 (2001).
- <sup>3</sup>A. El-Habachi and K. H. Schoenbach, Appl. Phys. Lett. **72**, 22 (1998).
- <sup>4</sup>P. Kurunczi, J. Lopez, H. Shah, and K. Becker, Int. J. Mass. Spectrom. **205**, 277 (2001).
- <sup>5</sup>J. W. Frame and J. G. Eden, Electron. Lett. **34**, 1529 (1998).
- <sup>6</sup>K. H. Schoenbach, A. El-Habachi, M. M. Moselhy, W. Shi, and R. H. Stark, Phys. Plasmas **7**, 2186 (2000).

- <sup>7</sup>M. Moselhy, W. Shi, R. H. Stark, and K. H. Schoenbach, Appl. Phys. Lett. **79**, 1240 (2001).
- <sup>8</sup>P. Kurunczi, H. Shah, and K. Becker, J. Phys. B **32**, L651 (1999).
- <sup>9</sup>M. Moselhy, W. Shi, R. H. Stark, and K. H. Schoenbach, IEEE Trans. Plasma Sci. **30**, 198 (2002).
- <sup>10</sup>M. Moselhy, I. Petzenhauser, K. Frank, and K. H. Schoenbach, J. Phys. D **36**, 2922 (2003).
- <sup>11</sup>K. H. Schoenbach, M. Moselhy, and W. Shi, Plasma Sources Sci. Technol. (to be published).
- <sup>12</sup>L. D. Biborosch, O. Bilwatsch, S. Ish-Shalom, E. Dewald, U. Ernst, and K. Frank, Appl. Phys. Lett. **75**, 3926 (1999).
- <sup>13</sup>J. D. Cobine, *Gaseous Conductors: Theory and Engineering Applications* (Dover, New York, 1958), pp. 218–225.
- <sup>14</sup>P. Gill and C. E. Webb, J. Phys. D **10**, 299 (1977).
- <sup>15</sup>M. Moselhy, R. H. Stark, K. H. Schoenbach, and U. Kogelschatz, Appl. Phys. Lett. **78**, 880 (2001).
- <sup>16</sup>A. El-Habachi and K. H. Schoenbach, Appl. Phys. Lett. **73**, 885 (1998).
- <sup>17</sup>K. H. Schoenbach, A. El-Habachi, W. Shi, and M. Ciocca, Plasma Sources Sci. Technol. **6**, 468 (1997).
- <sup>18</sup>B. Gellert and U. Kogelschatz, Appl. Phys. B: Photophys. Laser Chem. **B52**, 14 (1991).
- <sup>19</sup>A. v. Engel and M. Steenbeck, *Elektrische Physik u. Technik* (Springer, Berlin, 1932 and 1934), Vols. 1 and 2.
- <sup>20</sup>Yu. D. Korolev and G. A. Mesyats, *Physics of Pulsed Breakdown in Gases* (Ural Division of the Russian Academy of Sciences, YeKaterinburg, 1998).
- <sup>21</sup>E. E. Kunhardt, IEEE Trans. Plasma Sci. **28**, 189 (2000).
- <sup>22</sup>Y. S. Akishev, A. A. Deryugin, I. V. Kochetov, A. P. Napartovich, and N. I. Trushkin, J. Phys. D **26**, 1630 (1993).
- <sup>23</sup>R. J. Carman and R. P. Mildren, J. Phys. D **36**, 19 (2003).
- <sup>24</sup>J. Galy, K. Aouame, A. Birot, H. Brunet, and P. Millet, J. Phys. B **26**, 477 (1993).
- <sup>25</sup>T. D. Bonifield, F. H. K. Rambow, G. K. Walters, M. V. McCusker, D. C. Lorents, and R. A. Gutcheck, J. Chem. Phys. **72**, 2914 (1980).
- <sup>26</sup>J. D. Ametepe, J. Diggs, D. M. Manos, and M. J. Kelley, J. Appl. Phys. **85**, 7505 (1999).